The 24th International Electronic Conference on Synthetic Organic Chemistry
15 Nov - 15 Dec 2020

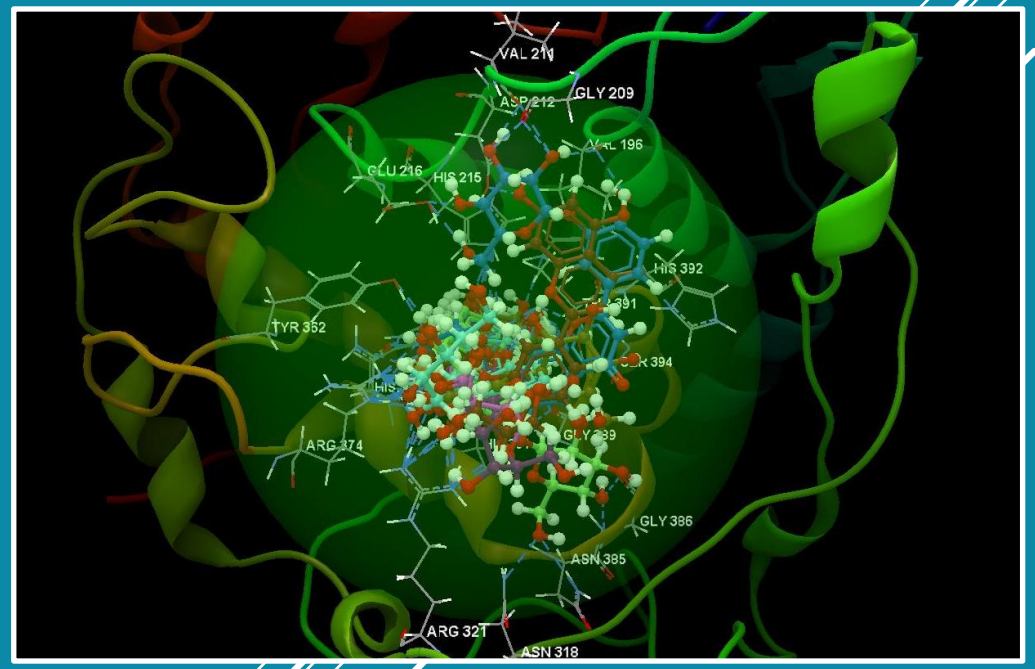

STOKESIA LAEVIS ETHANOLIC EXTRACT ACTIVITY ON THE NORMAL AND MALIGNANT MURINE CELL LINE VIABILITY L969 AND B16

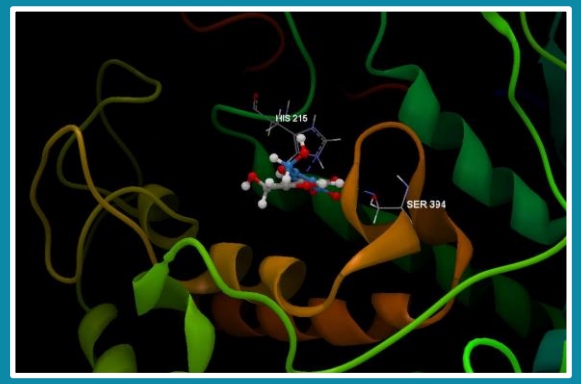

Georgeta Neagu, Amalia Stefaniu, Bujor Albu,

Iulian Terchescu, Lucia Pintilie and Lucia Pirvu*

National Institute for Chemical-Pharmaceutical Research and Development,
112 Vitan Av., 031299 Bucharest, Romania
*Correspondence: lucia.pirvu@yahoo.com

AIM

The present paper aims to study the cytotoxic and anti-proliferative potential of the standardized ethanolic extract (Slae26) from *Stokesia laevis* (J. Hill, fam. *Asteraceae*), 5 mg GAE/mL extract, on normal murine fibroblast cell line L929 and malignant murine melanoma cell line B16, respectively.

METHODS

The in vitro cytotoxicity and anti-proliferative assays were done according to the Technical Bulletin of Promega Corporation CellTiter 96 AQueous One solution Cell Proliferation Assay.

The molecular docking study was realized using CLC Drug, Discovery Work Bench. Protein fragment, human tyrosinase related protein 1 in complex with kojic acid (PDB ID 5M8M).
Ligands: Caffeic acid, Chlorogenic acid, Luteolin, Luteolin-5-O-glucoside, Luteolin-7-O-glucoside, Luteolin-6-C-glucoside, Luteolin-8-C-glucoside, Luteolin-7,3'-di-O-glucoside and Luteolin 3,4’-di-O-glucoside) were docked into 107.01 $Å^3$ binding pocket of 5M8M fragment.

RESULTS

Cytotoxicity and anti-proliferative assays

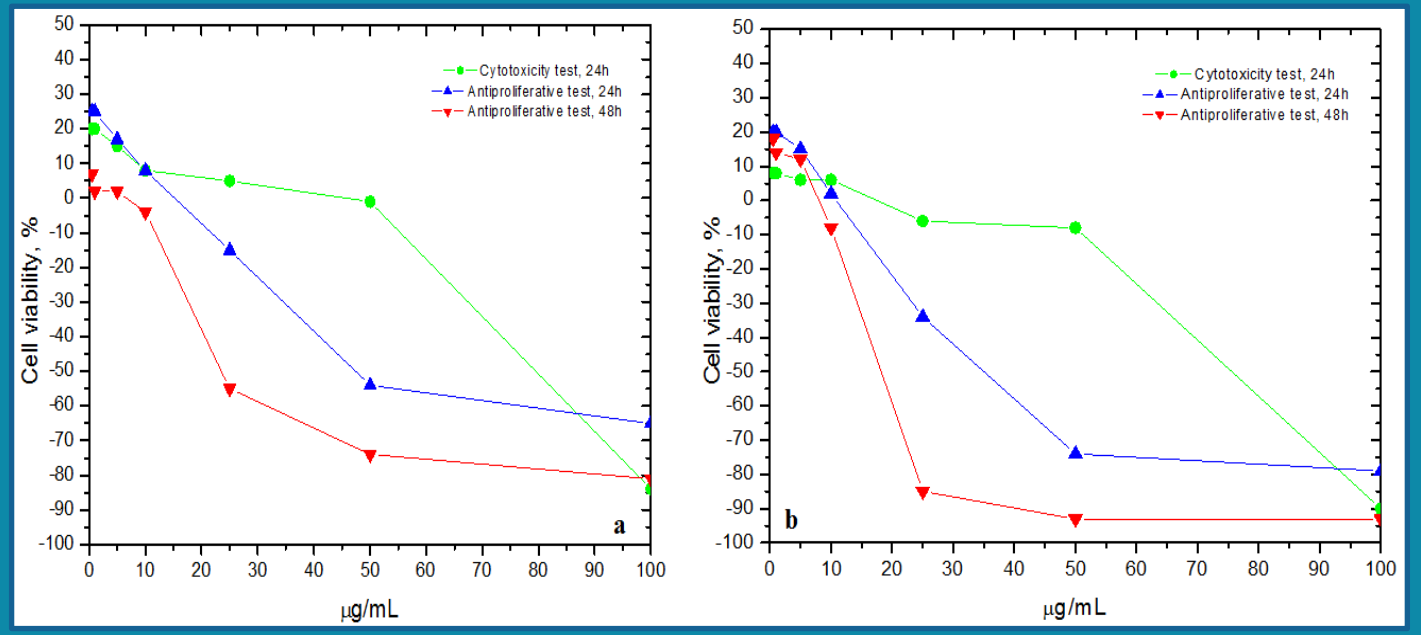

Fig. 1. Cytotoxic and antiproliferative effects (cell viability, %) of Slae26 dilution series tested on **(a)** murine fibroblast cell line L929 and (**b**) murine melanoma cell line B16, compared to control negative cell lines (40% ethanol solvent series); n = 3, ±SD (%)

RESULTS

Molecular docking results

Fig. 2. Structure of 5M8M (human tyrosinase related protein 1 in complex with Kojic acid).

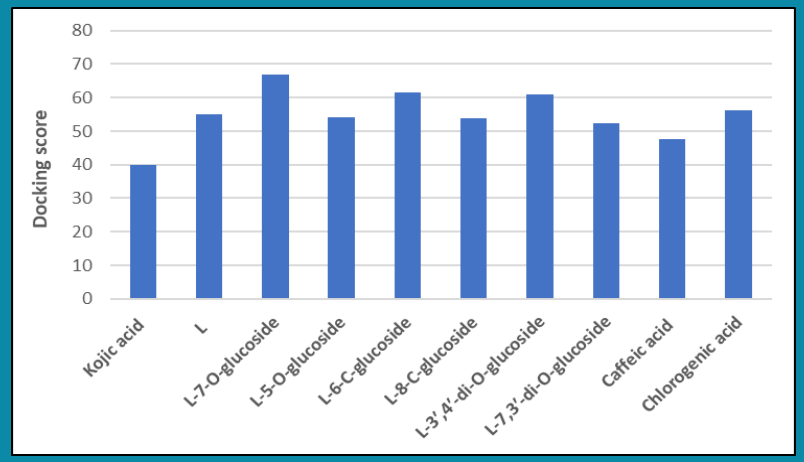

Fig. 3. Docking scores for Luteolin (**L**) derivatives, caffeic and chlorogenic acids, against human tyrosinase related protein 1 (PDB ID 5M8M).

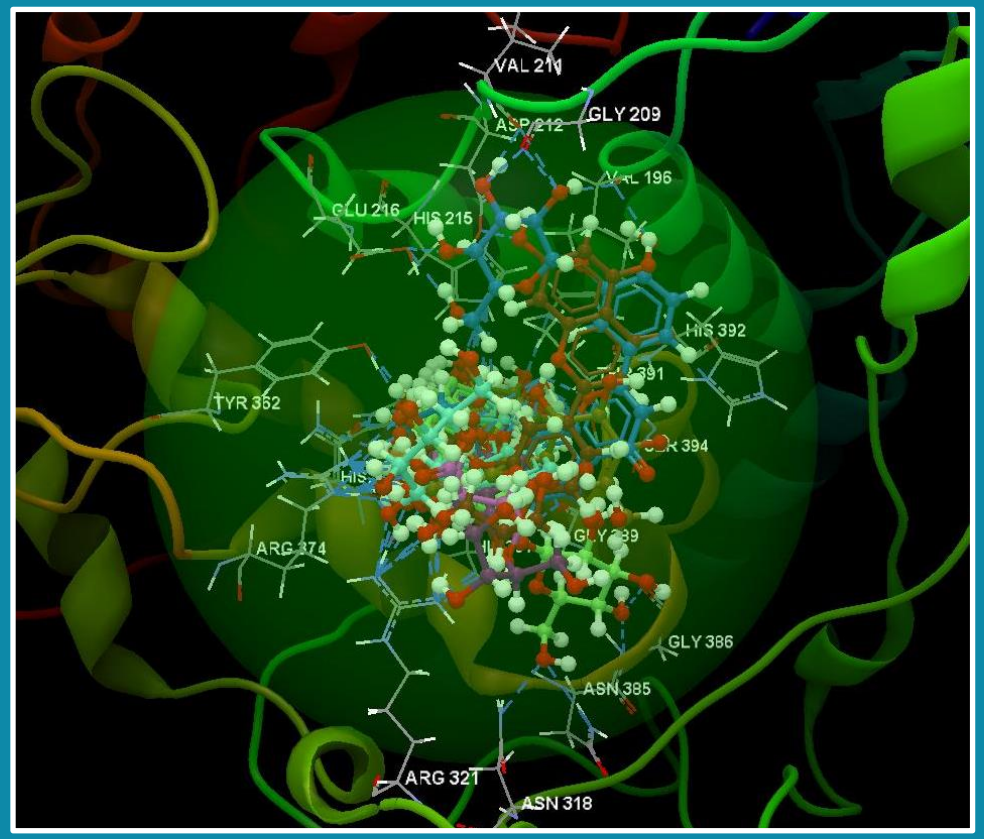

Fig. 4. 5M8M structure with co-crystallized and investigated ligands' interactions with amino acid residues form the active binding site

LIGANDS

- Caffeic acid,
- Chlorogenic acid,
- Luteolin (**L**)
- **L**-5-O-glucoside,
- **L**-7-O-glucoside,
- **L**-6-C-glucoside,
- **L**-8-C-glucoside,
- **L**-7,3'-di-O-glucoside
- **L**-3,4'-di-O-glucoside

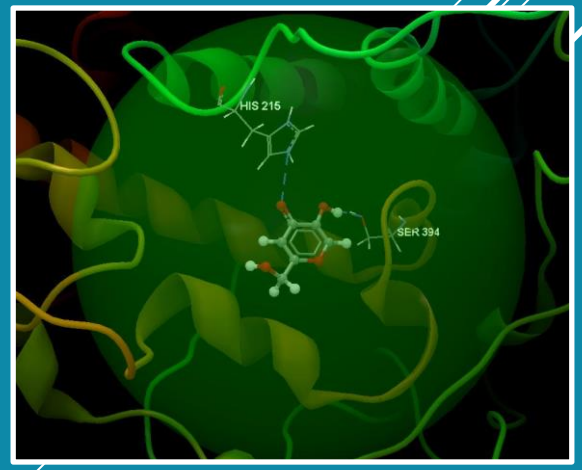

Fig. 5. Kojic acid's interactions and binding site

RESULTS

Molecular docking results for Luteolin

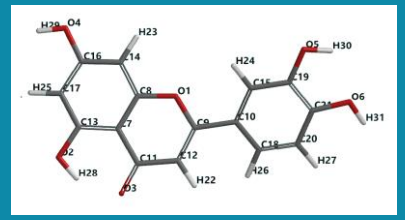

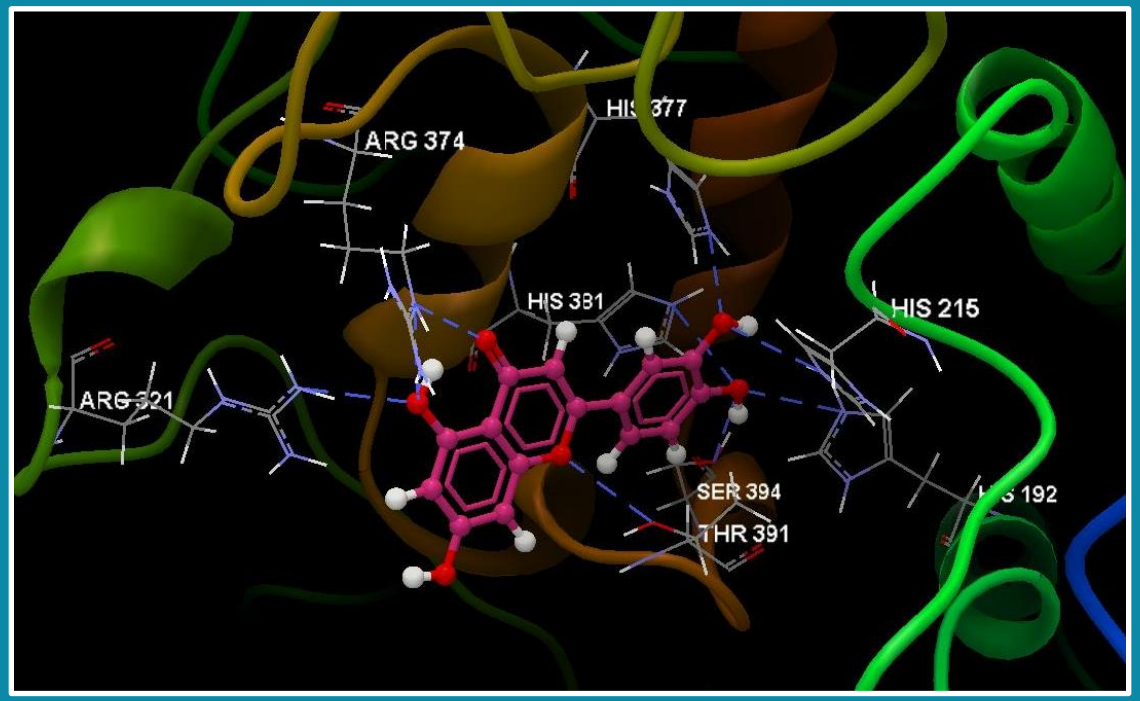

Fig. 6. Hydrogen bonds of L

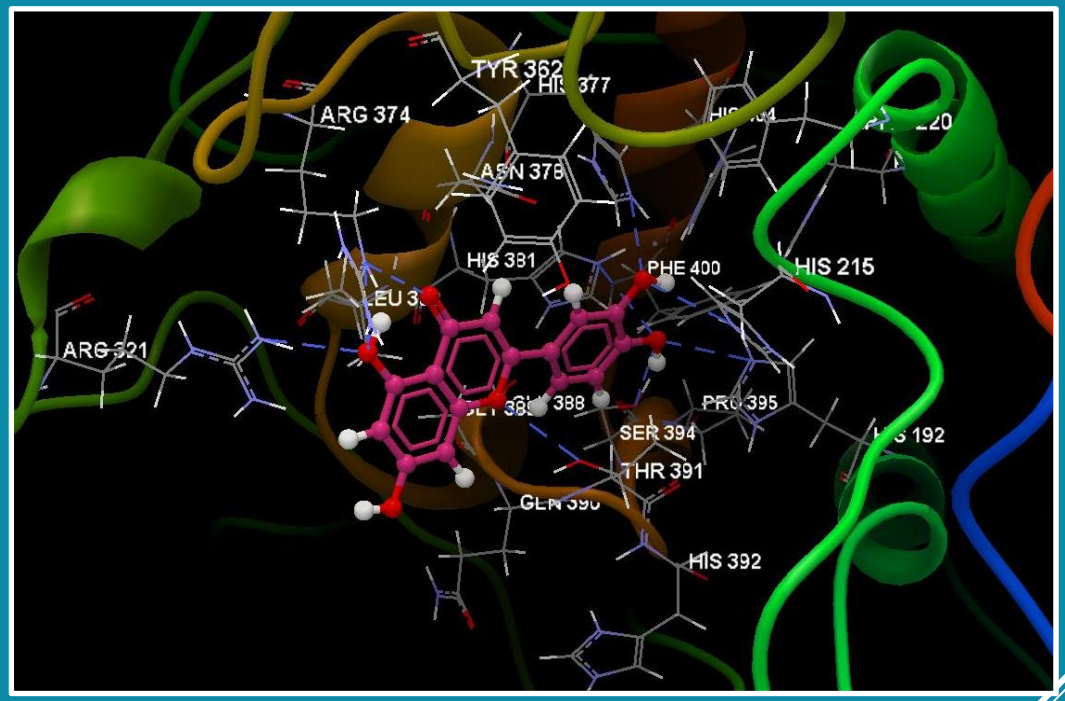

Fig. 7. interacting group and Hydrogen bonds of L

Interacting group (chain A)
ARG374, TYR362, HIS377, HIS401, PHE220, HIS224, ARG321, LEU382, ASN378, HIS381, PHE400, HIS215, HIS192, PRO395, SER394, GLY388, GLY389, THR391, GLN390, HIS392

SCORE: 55.02 RMSD: 0.02

Osp² (O3) - Nsp² ARG374	2.969 Å
Osp³ (O2) - Nsp² ARG374	2.846 Å
Osp ³(O2) - Nsp² ARG374	2.885 Å
Osp³ (O2) - Nsp² ARG321	3.174 Å
Osp² (O1) - Osp³ THR391	3.166 Å
Osp³ (O5) - Nsp² HIS377	2.982 Å
Osp³ (O5) - Nsp² HIS215	3.161 Å
Osp³ (O6) - Nsp² HIS192	3.134 Å
Osp³ (O6) - Osp³ SER394	2.968 Å
Osp³ (O6) - Nsp² HIS381	3.387 Å

RESULTS

Molecular docking results for L-7-O-glucoside

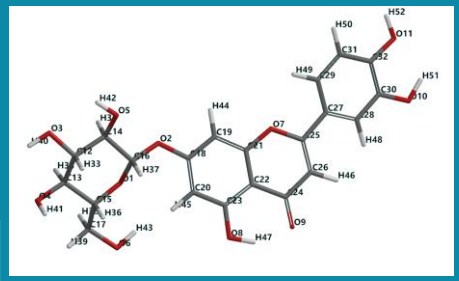

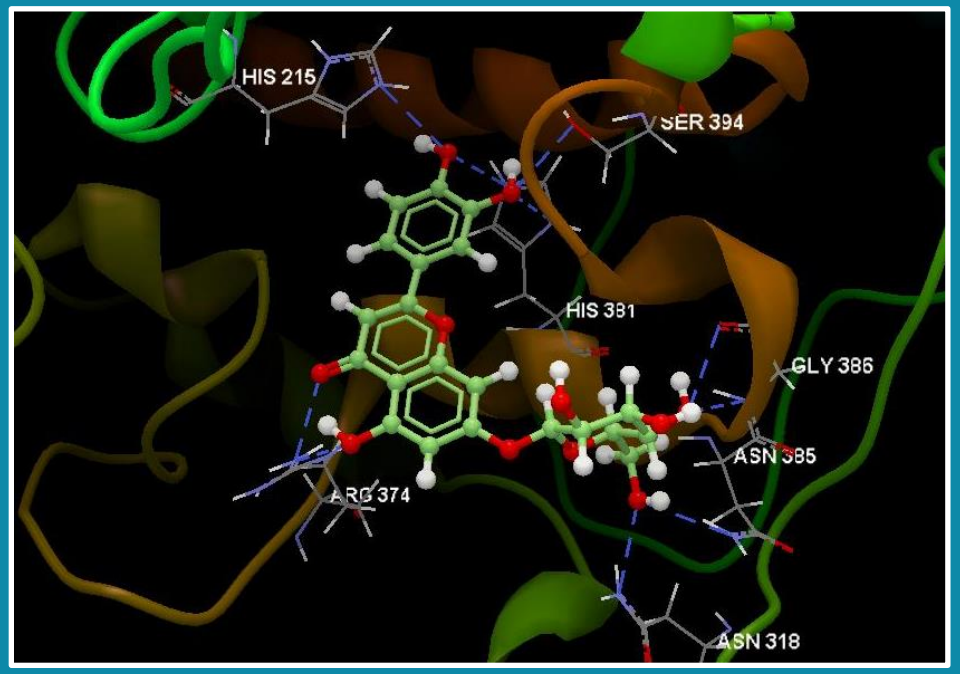

Fig. 8. Hydrogen bonds of L-7-O-glucoside

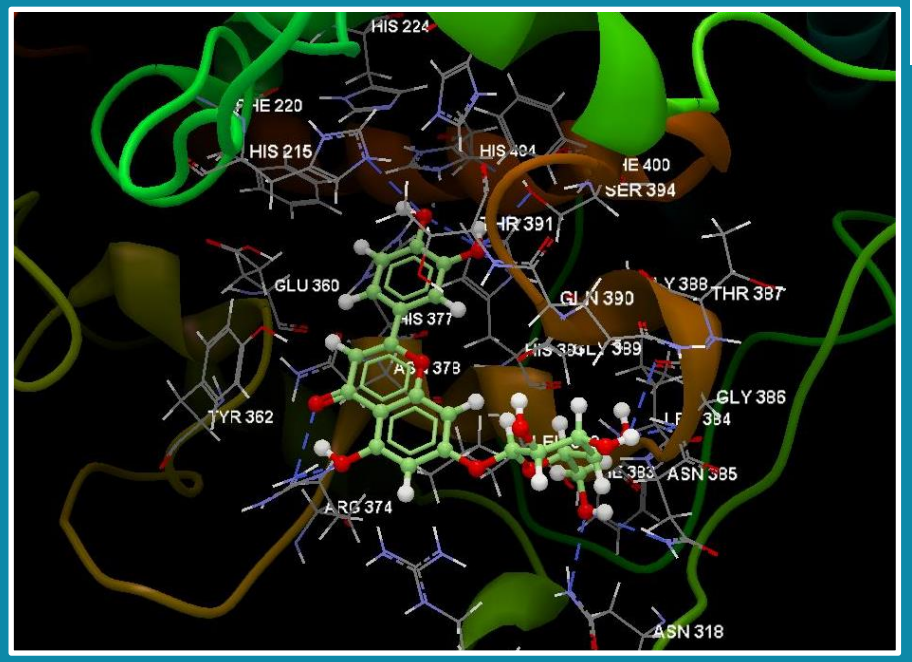

Fig. 9. interacting group and Hydrogen bonds of L-7-O-glucoside9

Interacting group (chain A)
HIS192, HIS224, PHE220, HIS215, HIS404, THR391, PHE400, SER394, GLU360, GLN390, GLY388, THR387, HIS377, ASN378, HIS381, GLY389, TYR362, ARG374, GLY386, LEU384, ASN385, LEU382, PHE383, ASN318, ARG321

SCORE: 66.76 RMSD: 1.27

Osp² (O9) - Nsp² ARG374	2.825 Å
Osp³ (O8) - Nsp² ARG374	2.552 Å
Osp³ (O6) - Nsp² ASN318	2.967 Å
Osp³ (O6) - Nsp² ASN385	3.103 Å
Osp³ (O4) - Nsp² GLY386	3.039 Å
Osp³ (O4) - Osp² GLY386	3.050 Å
Osp³ (O10) - Nsp² HIS381	3.173 Å
Osp³ (O10)- Osp³ SER394	2.906 Å
Osp³ (O11) - Nsp² HIS215	3.985 Å
Osp³ (O11) - Nsp² HIS381	3.084 Å

RESULTS

Molecular docking results for L-5-O-glucoside

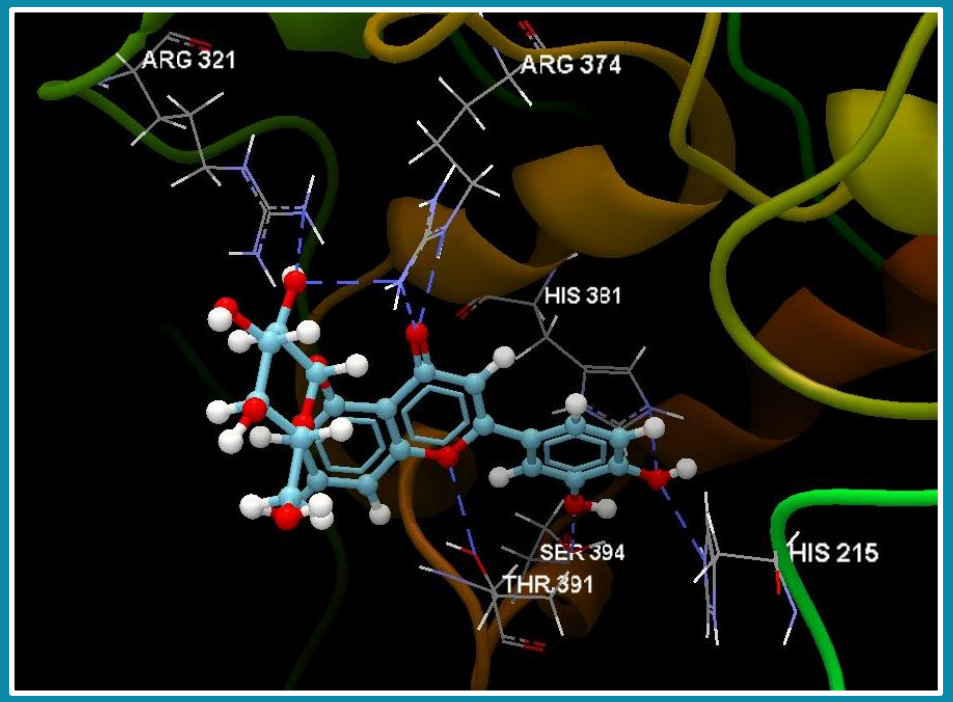

Fig. 10. Hydrogen bonds of L-5-O-glucoside

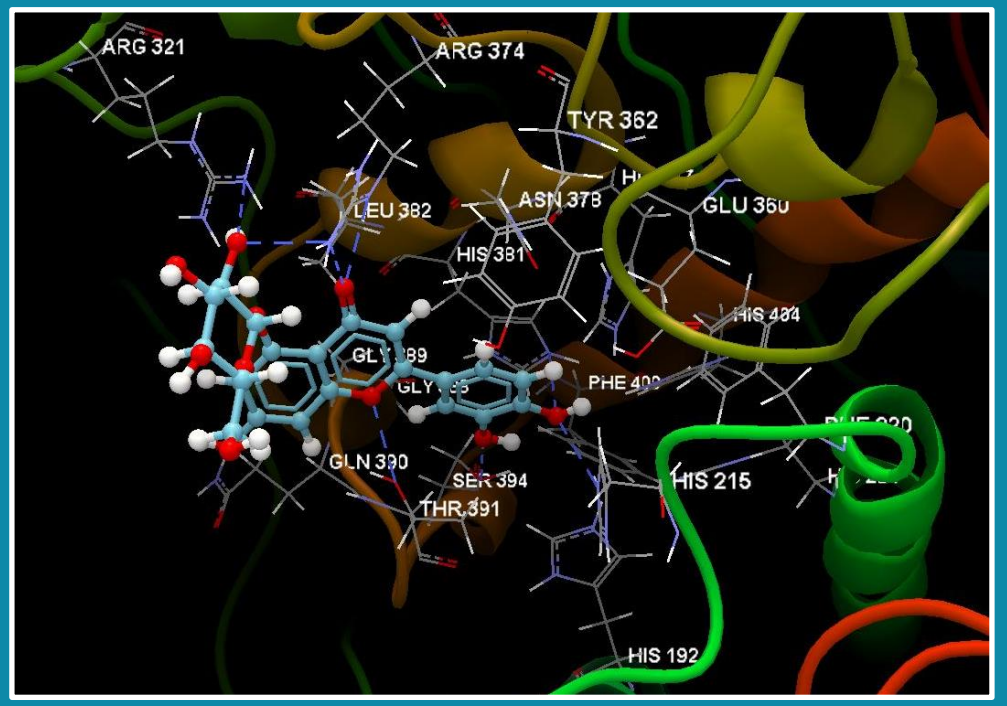

Fig. 11. interacting group and Hydrogen bonds of L-5-O-glucoside

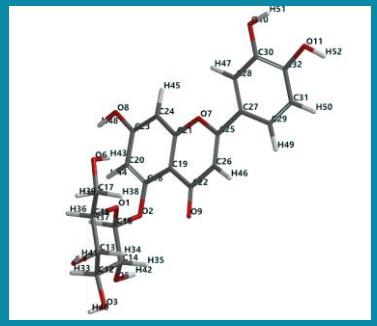

Interacting group (chain A)
ARG321, ARG374, LEU382, TYR362, ASN378, HIS381, HIS377, GLU360, HIS404, PHE220, HIS224, HIS192, HIS215, PHE400, THR391, SER394, GLN390, GLY388, GLY389

SCORE: 54.21 RMSD: 0.13

Osp^2 (O9) - Nsp^{2}ARG374	3.038 Å
Osp^2 (O9) - Nsp^{2}ARG374	3.030 Å
Osp^3(O5) - Nsp^{2}ARG374	2.820 Å
Osp^3(O5) - Nsp^{2}ARG321	2.713 Å
Osp^2(O7) - Osp^{3}THR391	2.744 Å
Osp^3(O11) - Nsp^{2}HIS215	3.103 Å
Osp^3(O11) - Nsp^{2}HIS381	3.225 Å
Osp^3(O10) - Osp^{3}SER394	2.642 Å

RESULTS

Molecular docking results for L-6-C-glucoside

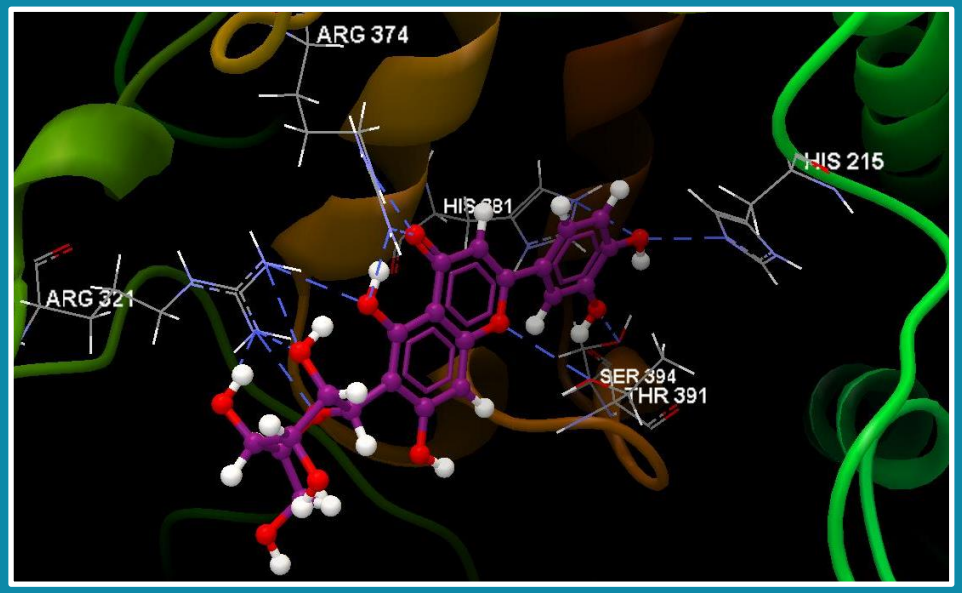

Fig. 12. Hydrogen bonds of L-6-C-glucoside

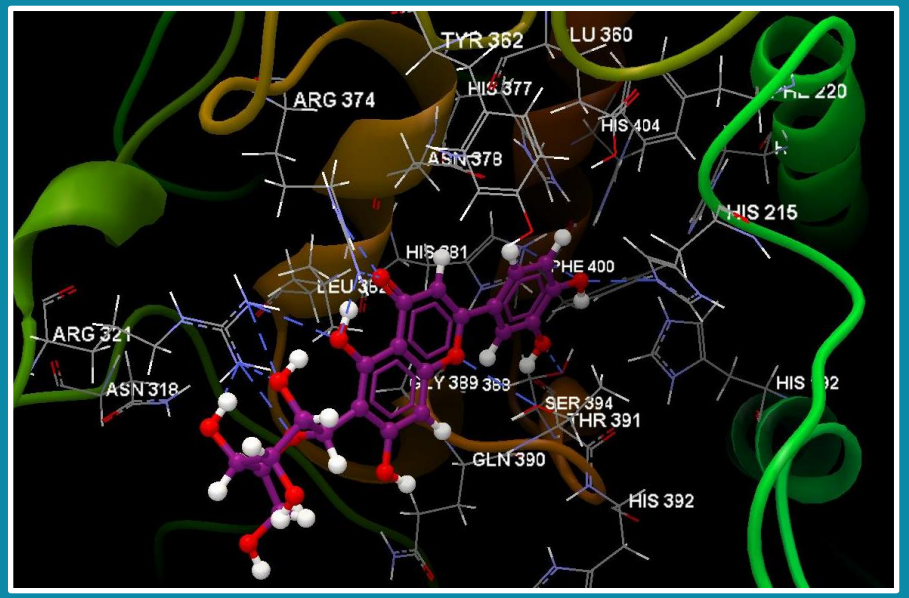

Fig. 13. interacting group and Hydrogen bonds of L-6-C-glucoside

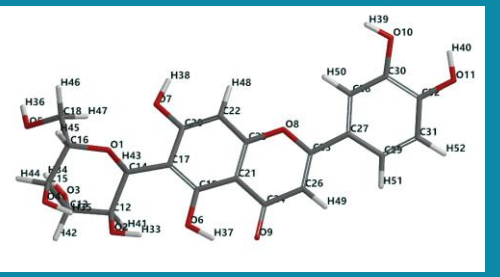

Interacting group (chain A)
ARG374, TYR362, GLU360, HIS377, ASN378, HIS404, PHE220, HIS224, HIS215, HIS192, HIS392, THR391, SER394, GLN390, GLY388, GLY389, HIS381, LEU382, ARG321, ASN318

SCORE: 61.55 RMSD: 0.15

Osp³(O9) - Nsp² ARG374	2.423 Å
Osp³(O9) - Nsp² ARG374	3.156 Å
Osp³(O6)-Nsp² ARG374	3.110 Å
Osp³(O6) - Nsp² ARG321	3.115 Å
Osp³(O2) - Nsp² ARG321	2.990 Å
Osp³(O2) - Nsp² ARG321	2.901 Å
Osp³(O1) - Nsp² ARG321	2.967 Å
Osp³(O4) - Nsp² ARG321	2.831 Å
Osp³(O10) - Osp³ SER394	2.502 Å
Osp³(O11) - Nsp² HIS381	3.248 Å
Osp³(O11) - Nsp²HIS215	3.113 Å
Osp²(O8) - Osp³THR391	3.180 Å

RESULTS

Molecular docking results for L-8-C-glucoside

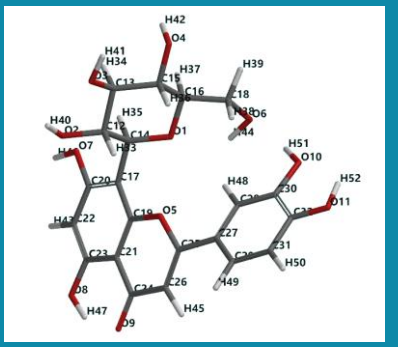

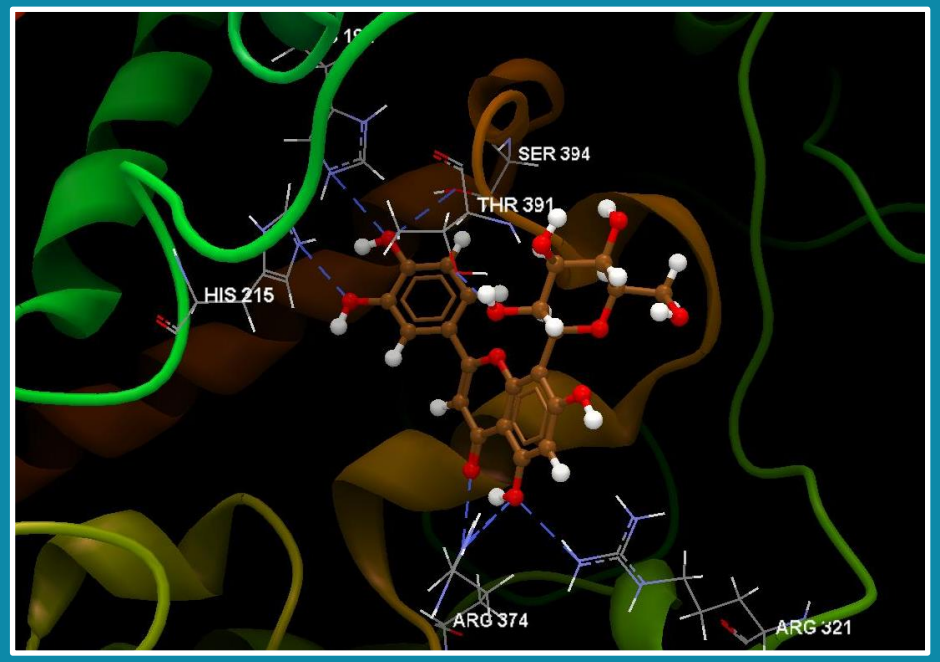

Fig. 14. Hydrogen bonds of L-8-C-glucoside

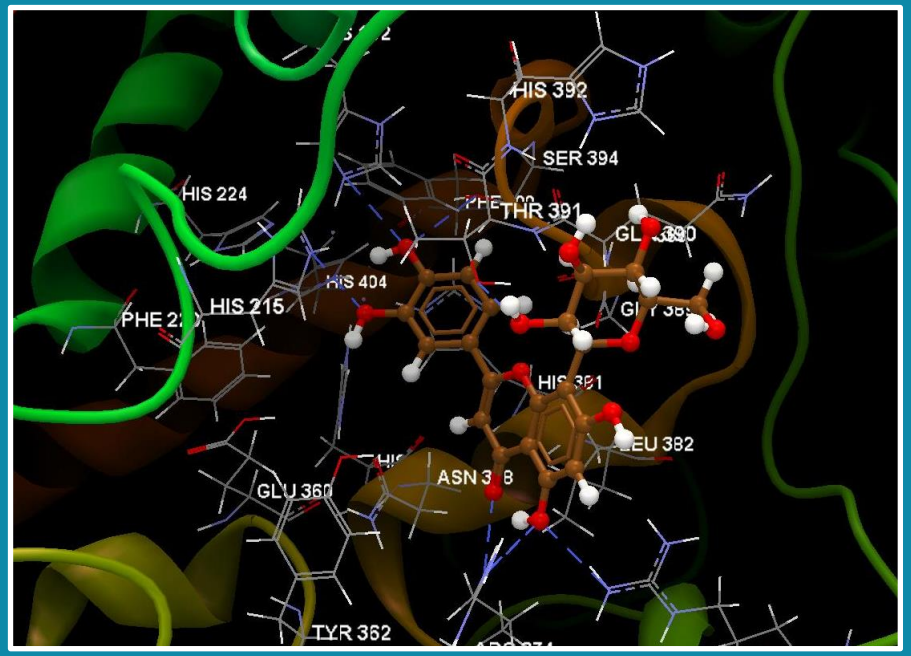

Fig. 15. interacting group and Hydrogen bonds of L-8-C-glucoside

Interacting group (chain A)
HIS192, HIS392, SER394, PHE400, THR391, GLN390, GLY388, GLY389, HIS381, LEU382, ARG321, ARG374, TYR362, ASN378, HIS377, GLU360, PHE220, HIS215, HIS204, HIS224

SCORE: 53.81 RMSD: 0.03

Osp² (O9) - Nsp²ARG374	2.884 Å
Osp² (O8) - Nsp²ARG374	2.569 Å
Osp² (O8) - Nsp²ARG374	2.592 Å
Osp² (O8) - Nsp² ARG321	3.083 Å
Osp³ (O10) - Nsp² HIS215	2.751 Å
Osp³ (O11) - Nsp² HIS192	3.134 Å
Osp³ (O11) -Osp³ SER394	3.060 Å
Osp³ (O2) - Osp³ THR391	2.451 Å

RESULTS

Molecular docking results for L-3′,4′-di-O-glucoside

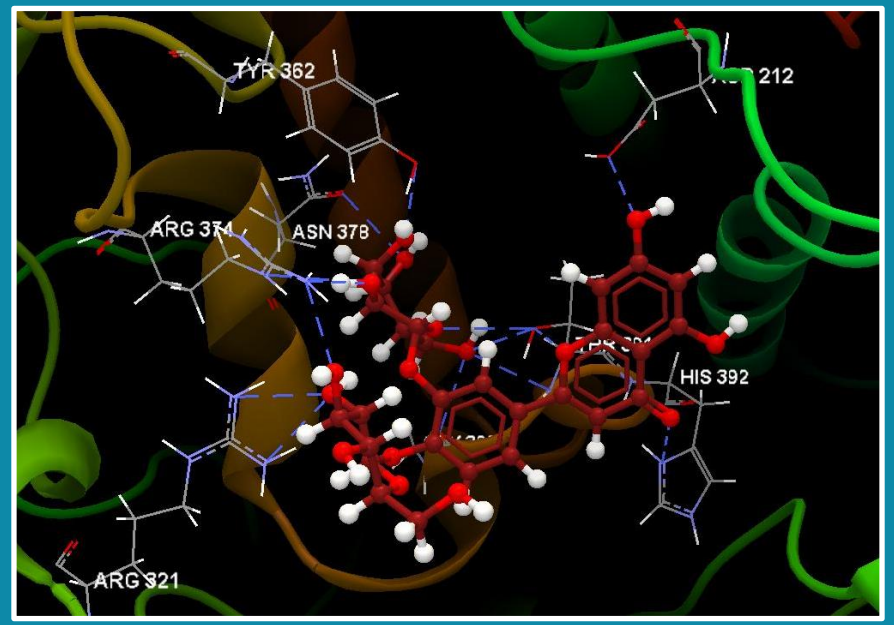

Fig. 16. Hydrogen bonds of L-3′,4′-di-O-glucoside

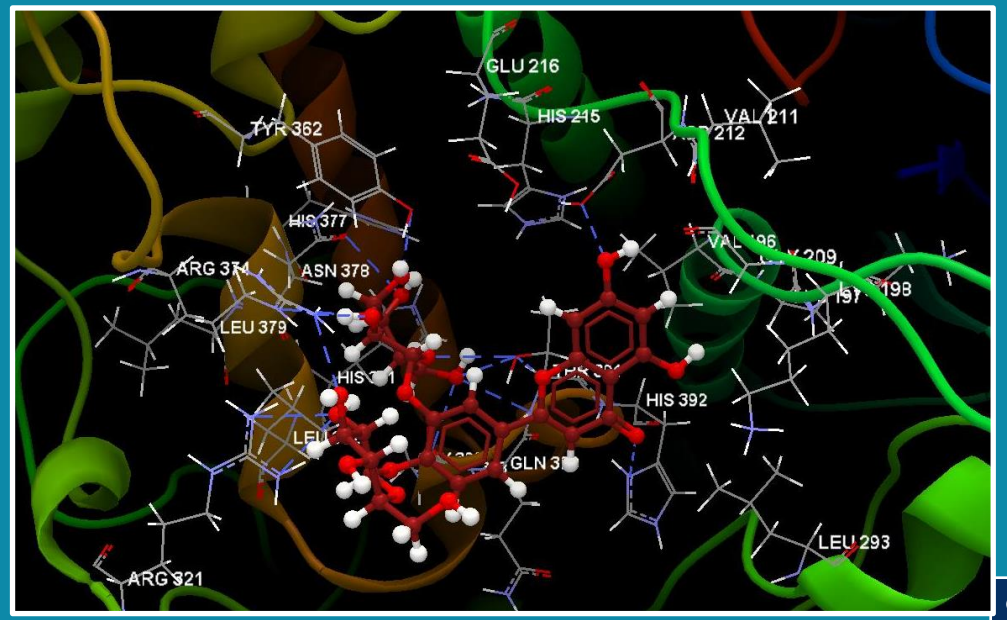

Fig. 17. interacting group and Hydrogen bonds of L-3′,4′-di-O-glucoside

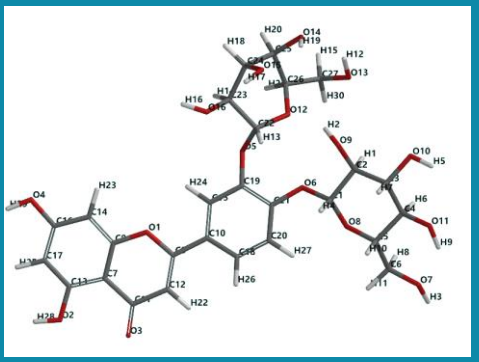

Interacting group (chain A)

GLU216, HIS215, ASP212, VAL211, VAL196, GLY209, LYS198, LYS197, LEU293, HIS392, THR391, GLN390, GLY388, GLY389, ARG321, LEU382, HIS381, LEU379, ASN378, ARG374, HIS377, TYR362

SCORE: 60.91 RMSD: 2.68

Osp^2 (O3) - Nsp^2 HIS392	2.789 Å
Osp^3 (O4) - Osp^3 ASP212	3.001 Å
Osp^2 (O1) - Osp^3 THR391	2.707 Å
Osp^3 (O12)-Osp^3 THR391	3.271 Å
Osp^3 (O13)-Osp^3 THR391	2.906 Å
Osp^3 (O13)-Nsp^2 THR391	3.050 Å
Osp^3 (O13)-Osp^2 GLY389	2.856 Å
Osp^3 (O14)-Osp^2 ASN378	3.046 Å
Osp^3 (O15)-Osp^3 TYR362	2.656 Å
Osp^3 (O16)-Nsp^2 ARG374	3.307 Å
Osp^3 (O16)-Nsp^2 ARG374	2.671 Å
Osp^3 (O9)-Nsp^2 ARG321	3.022 Å
Osp^3 (O9)-Nsp^2 ARG321	2.909 Å
Osp^3 (O10)-Nsp^2 ARG374	3.073 Å

RESULTS

Molecular docking results for L-7, 3′-di-O-glucoside

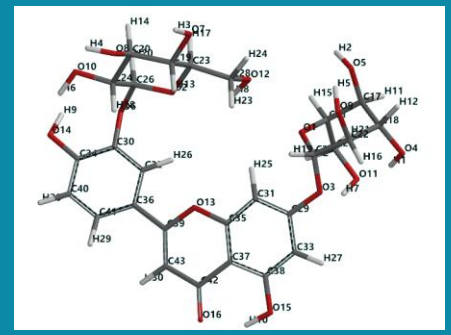

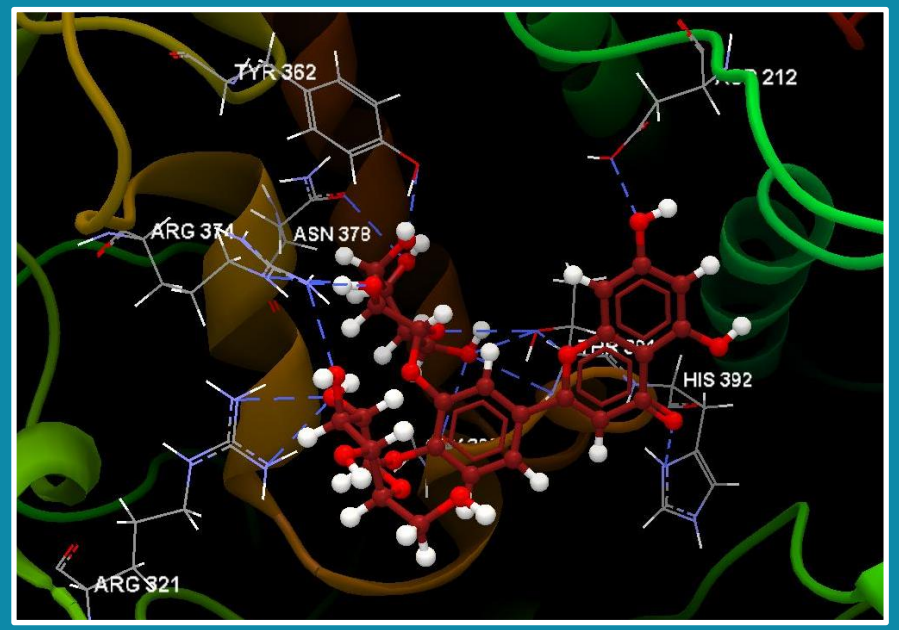

Fig. 18. Hydrogen bonds of L-7, 3′-di-O-glucoside

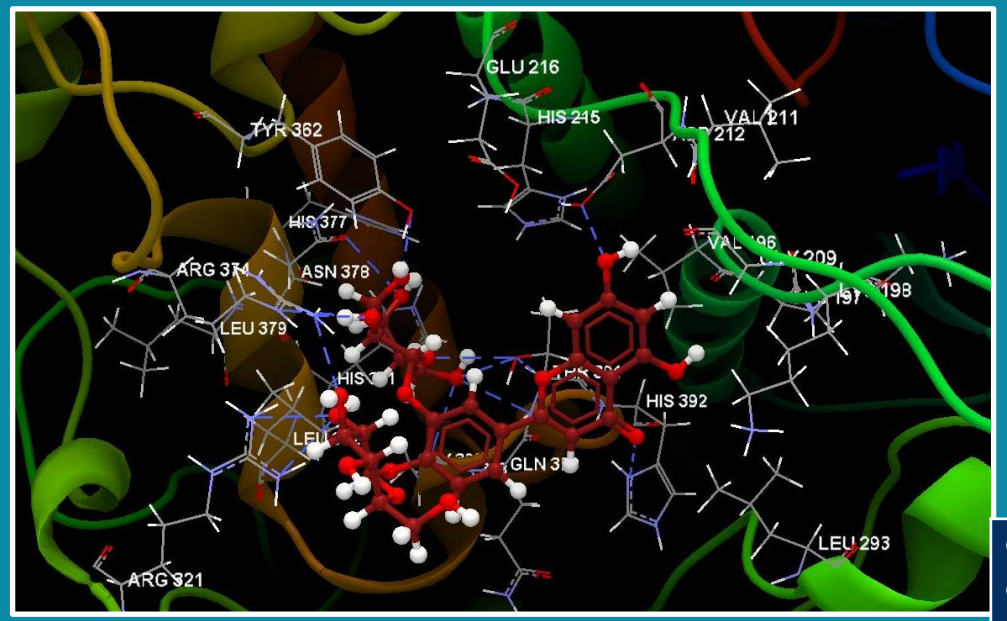

Fig. 19. interacting group and Hydrogen bonds of L-7, 3′-di-O-glucoside

Interacting group (chain A)

LEU293, HIS392, THR391, GLN390, GLY389, HIS381, LEU382, ARG321, ASN378, HIS377, ARG374, GLU360, TYR362, TYR348, GLU216, HIS215, GLU210, VAL211, ASP212, GLY209, VAL196, LYS198, LYS197

SCORE: 52.44 RMSD: 2.43

Osp² (O13)-Osp³ THR391	2.836 Å
Osp² (O13)-Nsp² THR391	3.192 Å
Osp³ (O14)-Osp² VAL196	2.698 Å
Osp³ (O10)-Osp² VAL196	3.094 Å
Osp³ (O10)-Osp² VAL211	2.913 Å
Osp³ (O10)-Osp² GLY209	3.240 Å
Osp³ (O8)-Osp² VAL211	2.867 Å
Osp³ (O8)-Osp² GLY209	2.823 Å
Osp³ (O7)-Osp³ GLU216	2.674 Å
Osp³ (O12)-Osp³ GLU216	3.054 Å
Osp³ (O1)-Osp³ THR391	3.157 Å
Osp³ (O5)-Osp³ TYR362	2.920 Å
Osp³ (O5)-Osp² ASN378	3.089 Å
Osp³ (O4)-Nsp² ARG374	3.148 Å
Osp³ (O4)-Nsp² ARG374	2.554 Å

RESULTS

Molecular docking results for caffeic acid

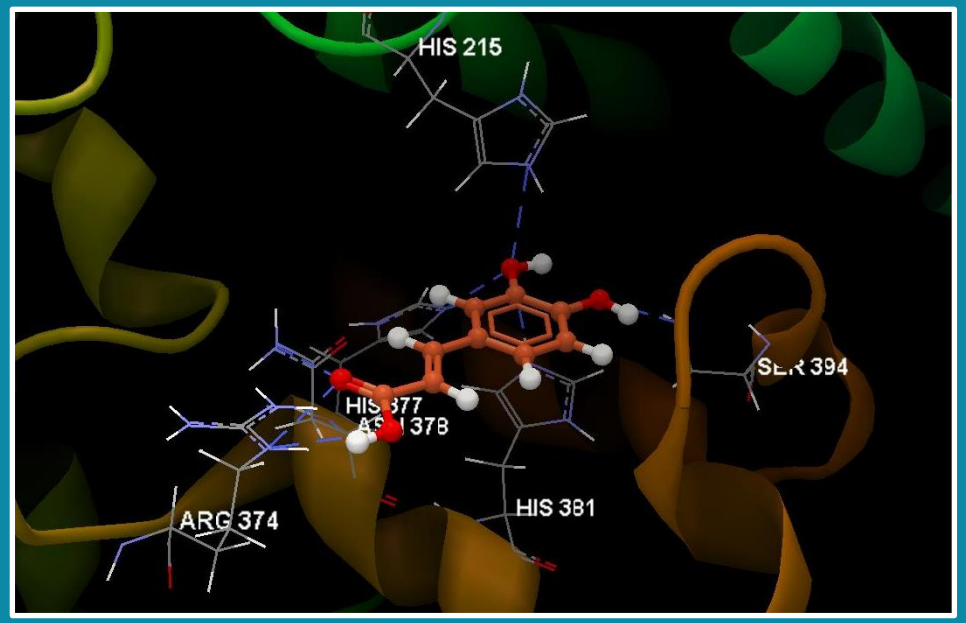

Fig. 20. Hydrogen bonds of caffeic acid

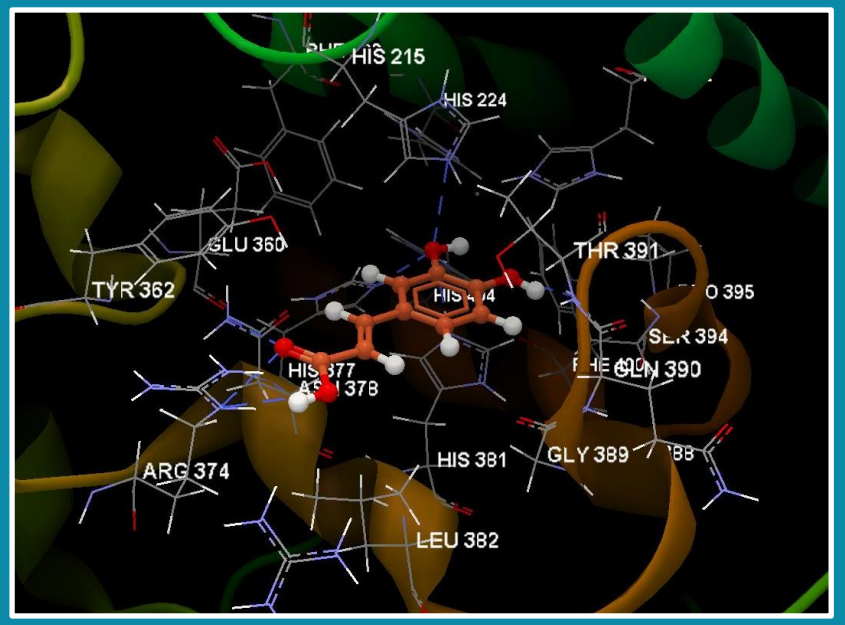

Fig. 21. interacting group and Hydrogen bonds of caffeic acid

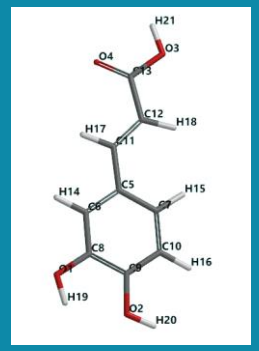

Interacting group (chain A)

PHE220, HIS215, HIS224, HIS192, THR391, PRO395, HIS404, SER394, PHE400, GLN390, GLY388, GLY389, LEU382, HIS381, ASN378, HIS307, ARG374, TYR362, GLU360

SCORE: 47.63 RMSD: 0.05

Osp^3 (O3)-Nsp^2 ARG374	3.146 Å
Osp^2 (O4)-Nsp^2 ARG374	2.860 Å
Osp^2 (O4)-Nsp^2 ASN378	3.034 Å
Osp^3 (O1)-Nsp^2 HIS377	3.195 Å
Osp^3 (O1)-Nsp^2 HIS215	3.019 Å
Osp^3 (O1)-Nsp^2 HIS381	3.374 Å
Osp^3 (O2)-Osp^3 SER394	2.424 Å

RESULTS

Molecular docking results for chlorogenic acid

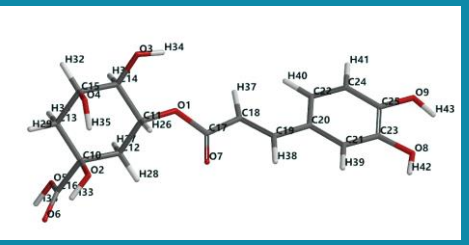

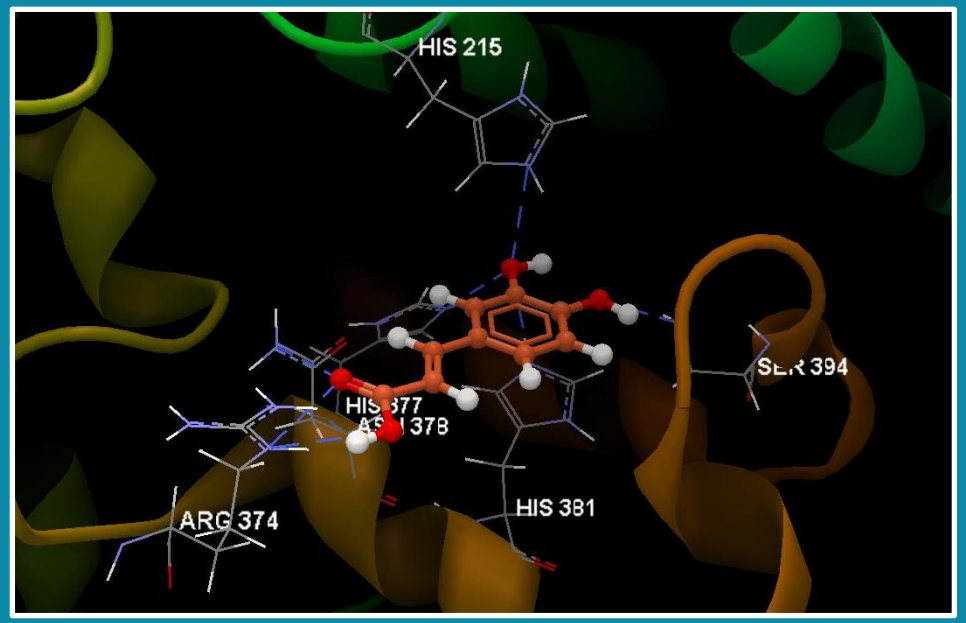

Fig. 22. Hydrogen bonds of chlorogenic acid

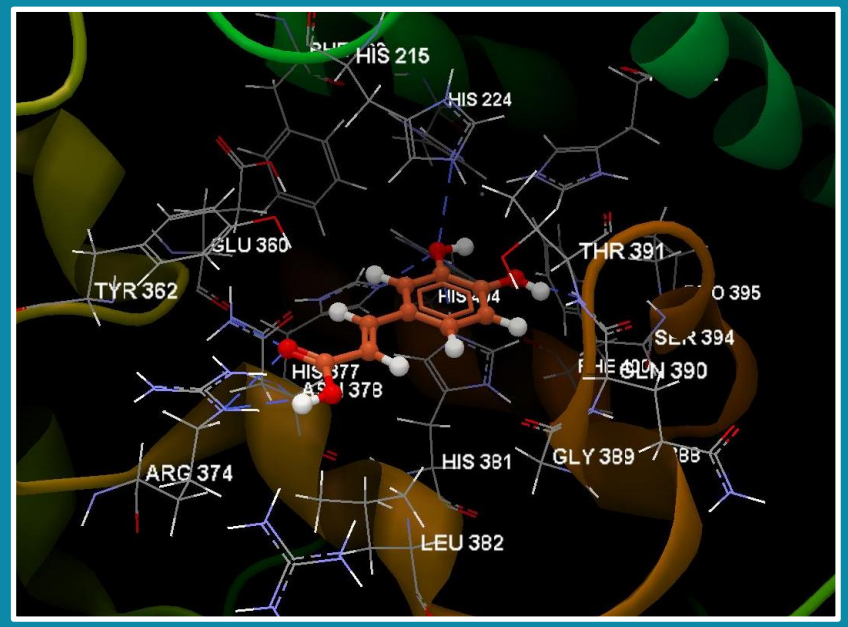

Fig. 23. interacting group and Hydrogen bonds of chlorogenic acid

Interacting group (chain A)

ARG321, ARG374, TYR362, LEU382, ASN378, HIS377, GLU360, HIS381, HIS404, PHE220, HIS224, **HIS215**, PHE400, GLY389, GLY388, GLN390, **SER394**, THR391, PRO395, HIS192

SCORE: 56.08 RMSD: 2.05

Osp^3 (O9)-Nsp^2 HIS381	3.289 Å
Osp^3 (O9)-Nsp^2 HIS215	3.031 Å
Osp^3 (O8)-Osp^3 SER394	2.523 Å
Osp^2 (O7)-Nsp^2 ARG374	2.854 Å
Osp^2 (O7)-Nsp^2 ARG374	3.072 Å
Osp^3 (O2)-Nsp^2 ARG321	3.107 Å
Osp^3 (O2)-Nsp^2 ARG321	2.738 Å
Osp^3 (O4)-Nsp^2 ARG321	2.862 Å
Osp^3 (O3)-Osp^2 GLY389	2.817 Å

Conclusions

The present work suggests certain cytotoxic and antiproliferative activity of 40% ethanolic extract (Slae26) from *Stokesia laevis* plant species (the aerial part), upon normal murine fibroblast cell line L929 and murine melanoma cell line B16; polyphenols compounds in Slae26 (HPTLC analysis) are caffeic acid, chlorogenic acid and luteolin-7-O-glucoside.

The docking results indicated similar interactions for the co-crystallized kojic acid, and our studies ligands, with the same amino acid residues, by hydrogen bonds formed with O sp^3 of SER394, and N sp^2 of HIS215, respectively, except for di-glucosides. In addition, due to the numerous hydroxyl groups of our investigated structures, more interactions in the protein-complex occur and higher docking score are revealed.

For the first time in literature data, potential cytotoxic and anti-proliferative effects of the ethanolic extract from S. aster on both, normal murine fibroblast cell line L929, and murine melanoma cell line B16 have been proved. Molecular docking approach on the major components of Slae26 against human tyrosinase receptor has reveal possible melanogenesis inhibition.